Coordinated Anions Tune Z-Type Ligand Displacement from Colloidal CdSe and InP Nanocrystal Surfaces

*Mawuli Degbevi, Jonathan T. Stoffel, and Emily Y. Tsui**

Department of Chemistry and Biochemistry, University of Notre Dame, Notre Dame, IN 46556

ABSTRACT. Neutral metal salts coordinate to the surfaces of colloidal semiconductor nanocrystals (NCs) by acting as Lewis acid acceptors for the NC surface anions. This ligand coordination has been associated with increased emission due to passivation of surface hole traps. Here, variation of the anionic ligands of metal salts is used to study anion effects on metal complex Lewis acidity and surface coordination at CdSe and InP NCs. To resolve dynamic ligand exchange processes, the tetracarbonylcobaltate anion, $[Co(CO)_4]^-$, is used as a monoanionic ligand for which IR spectroscopy can readily identify displacement of neutral $M[Co(CO)_4]_x$ species (M = Cd or In; x = 2 or 3, respectively) upon addition of neutral donor ligands. Notably, although $Cd[Co(CO)_4]_2$ is more Lewis acidic than cadmium oleate, the former is more readily displaced from the NC surfaces. Lewis acidity and X-type anion exchange are therefore factors to be considered when performing post-synthetic addition of metal salts for NC photoluminescence emission enhancement.

INTRODUCTION

Ligand coordination to the surfaces of colloidal semiconductor nanocrystals (NCs) contributes to NC colloidal stability and passivation of surface traps for improved photoluminescence quantum yield (PLQY).[1-4] NC surface ligands have been categorized based on Green's covalent bond classification scheme: X-type ligands are anionic donors like carboxylates, halides, and phosphonates, L-type ligands are neutral Lewis basic donors like amines and phosphines, and Z-type ligands are Lewis acidic compounds like metal salts (e.g. metal carboxylates, metal halides, etc.).[5-6] The addition of Z-type ligands has been identified as an effective method for passivating surface hole traps of metal chalcogenides (e.g. CdSe, CdTe) and InP NCs by coordination of low-coordinate surface anions.[1, 3-4, 7]

NC surfaces exhibit multiple ligand binding, dissociation and displacement equilibria, two examples of which are shown in Scheme 1. In the first (Scheme 1A), surface-bound Z-type MX_n ligands can be coordinated by additional donors (L) that result in Z-type ligand displacement and removal of a metal complex from the NC surface. This process is termed L-type-assisted Z-type displacement. The second example shows that anions that are only weakly coordinated to surface metal ions can themselves dynamically exchange via X-type dissociation. This dynamic behavior can make sample characterization challenging. ^{1}H NMR spectroscopy has been a primary method for studying these processes, as the resonances of NC-bound ligands (e.g., the alkenyl protons of oleate [OA^-]) are broadened and shifted compared to that of oleic acid (HOA), free OA^- anions, or molecular oleate-containing species like metal oleate complexes.[8-10] The latter three species all exhibit sharp ^{1}H NMR resonances at similar chemical shifts, however, meaning that the dissociation or displacement of L-, X-, or Z-type ligands from NC surfaces can be difficult to deconvolute if all three reactions occur simultaneously.

Scheme 1. Examples of ligand exchange reactions at NC surfaces.

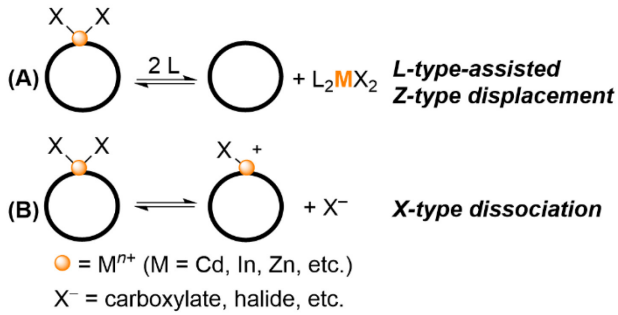

We have previously demonstrated that the native carboxylate ligands of OA^--capped CdSe and CdS NCs (CdSe-$Cd(OA)_2$ and CdS-$Cd(OA)_2$ NCs, respectively) can be exchanged for dianionic or monoanionic metal carbonyl fragments ($[M(CO)_4]^{n-}$, M = Fe and Co, n = 2 and 1, respectively) to form the resulting $[M(CO)_4]^{n-}$-functionalized NCs.[11-12] $[Fe(CO)_4]^{2-}$ moieties can also be attached to the NC surfaces by addition of the heterobimetallic precursor $(NH_3)_2CdFe(CO)_4$, which adds a $[CdFe(CO)_4]$ unit as a Z-type ligand.[13] The C–O stretching vibrations of the surface-bound $[Fe(CO)_4]^{2-}$ exhibit distinct bands in the IR spectra of the NC samples (ν_{CO} bands), enabling their use as spectroscopic reporters of NC surface reactions. Although the addition of Lewis bases like THF, octylamine, or *N,N,N′,N′*-tetramethylethylenediamine (TMEDA) removes the $[CdFe(CO)_4]$ unit via L-type-assisted Z-type ligand displacement under certain conditions, strongly-bound populations of $[CdFe(CO)_4]$ remain attached to CdSe NC surfaces even in the presence of excess Lewis base.[13]

In this work, the effects of anion substitution upon Z-type ligand displacement and binding of cadmium and indium salts at CdSe and InP NC surfaces are examined. Metal salts with more electron-poor anions are shown to be more readily displaced from NC surfaces by Lewis bases like THF, phosphines, and amines. Comparison of $Cd[Co(CO)_4]_2$ and $In[Co(CO)_4]_3$ addition to

both CdSe and InP NCs indicates that $[Co(CO)_4]^-$ transfer from In^{3+} to Cd^{2+} is facile and is driven by the relative energies of the Cd–X and In–X bonds, where X^- = $[Co(CO)_4]^-$ and OA^-. Photoluminescence (PL) measurements were used to compare Z-type ligand binding of $Cd[Co(CO)_4]_2$, $Cd(O_2CCF_3)_2$, and $Cd(OA)_2$ salts to CdSe NCs. Altogether, these studies demonstrate that both the metal cation and the anion must be considered together during the design of Z-type ligands for improved NC surface passivation.

RESULTS AND ANALYSIS

Synthesis and characterization. A sample of $[Co(CO)_4]^-$-functionalized CdSe NCs (CdSe-$Cd[Co(CO)_4]_2$ NCs, d ~ 3.8 nm, d is the NC diameter) was prepared by heating a toluene mixture of zinc blende CdSe-$Cd(OA)_2$ NCs and $Et_3SiCo(CO)_4$ (50 equiv/NC) at 80 °C for 5 h (Scheme 2A).[12] This reaction performs X-type exchange of the native oleate ligands for $[Co(CO)_4]^-$, forming Et_3SiOA as the byproduct. Purification by gel permeation chromatography (GPC)[14] to remove Et_3SiOA and other byproducts yielded the samples of CdSe-$Cd[Co(CO)_4]_2$ NCs. Electronic absorption spectroscopy (Fig. 1A) and transmission electron microscopy (TEM, Figs. S5, S6) show that the resulting NCs are mostly unchanged in size from the as-prepared CdSe-$Cd(OA)_2$ NC sample. These samples were further characterized by inductively-coupled plasma optical emission spectroscopy (ICP-OES) and ^1H NMR spectroscopy to quantify the surface concentrations of bound $[Co(CO)_4]^-$ (48 Co/NC, 1.1 Co/nm^2) and remaining OA^- ligands (80 OA^-/NC, 1.9 OA^-/nm^2), respectively.

Scheme 2. (A) Synthesis of CdSe-$Cd[Co(CO)_4]_2$ NCs. (B) Synthesis of InP-$In[Co(CO)_4]_3$ NCs. Oleylamine (not shown) is also coordinated to the InP NC surface. For clarity, only one anion (Cl^- or $[Co(CO)_4]^-$) is shown coordinated to the NC surface, but three anions are required for charge balance.

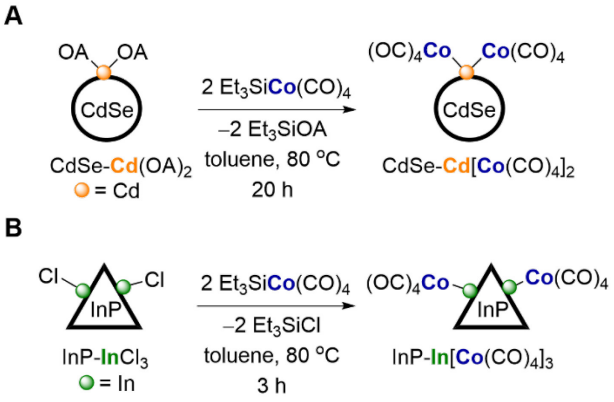

$[Co(CO)_4]^-$-functionalized InP NCs were prepared following a similar method (Scheme 2B). Tetrahedral $OlNH_2$-capped InP NCs (l ~ 4.5 nm, $OlNH_2$ = oleylamine, l is the NC edge length) were prepared following previously published procedures.[15] The presence of Cl^- as charge-balancing anions for InP NCs prepared using this method has been previously measured by XPS, although these surface densities were not quantified.[16-17] Treatment of these as-prepared InP-$InCl_3$ NCs with $Et_3SiCo(CO)_4$ at 80 °C for 3 h followed by GPC purification allowed isolation of a product nominally assigned as InP-$In[Co(CO)_4]_3$ NCs, although the precise coordination sphere and charge-balancing of the surface In^{3+} sites in these InP NCs is unclear.[18-19] This X-type ligand exchange reaction is presumed to proceed by exchange of chloride ligands for $[Co(CO)_4]^-$ to release Et_3SiCl as a byproduct. ^{1}H NMR spectroscopy of the as-prepared and functionalized InP NCs shows ca. 43±12 $OlNH_2$/NC (1.2 nm^{-2}), meaning that $OlNH_2$ ligands are not removed by this functionalization procedure. Electronic absorption spectroscopy shows a small blue shift (ca. 40 meV) in the excitonic absorption band after surface functionalization (Fig. 1B), although no size differences were observed by TEM (Figs. S10, S11).

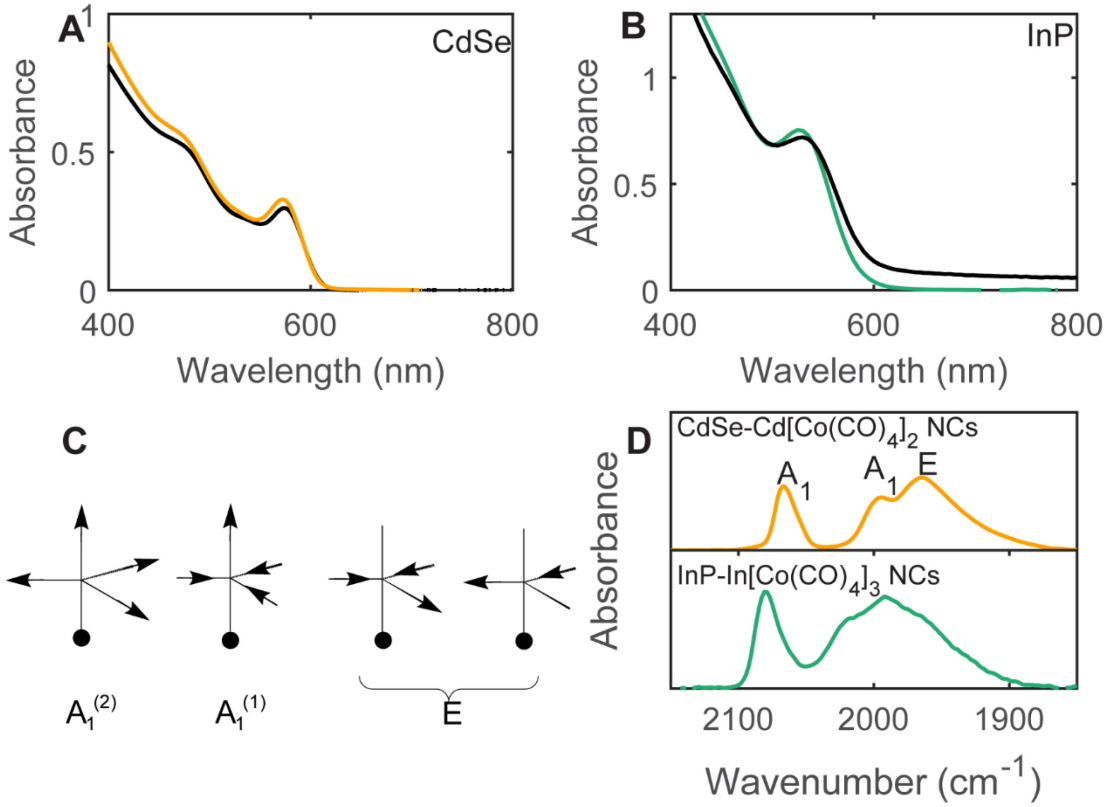

Figure 1. (A) Electronic absorption spectra of toluene suspensions of as-prepared CdSe-$Cd(OA)_2$ NCs ($d \sim 4.0$ nm, black) and CdSe-$Cd[Co(CO)_4]_2$ NCs (orange). (B) Electronic absorption spectra of toluene suspensions of as-prepared InP-$InCl_3$ NCs ($l \sim 4.5$ nm, black) and InP-$In[Co(CO)_4]_3$ NCs (green). (C) Schematic of C–O stretching modes for locally C_{3v}-symmetric trigonal bipyramidal $[M]Co(CO)_4$ fragments. (D) IR spectra (ν_{CO} region) of a hexanes suspension of CdSe-$Cd[Co(CO)_4]_2$ NCs ($d \sim 3.8$ nm, top) and of InP-$In[Co(CO)_4]_3$ NCs ($l \sim 4.5$ nm, bottom).

Figure 1D top shows the FTIR spectrum of a hexanes suspension of CdSe-$Cd[Co(CO)_4]_2$ NCs. This spectrum displays three ν_{CO} bands at 2067, 1996, and 1965 cm^{-1}, consistent with the expected three bands ($2A_1$ + E symmetry) for a locally C_{3v}-symmetric Cd-bound $[Co(CO)_4]^-$ species in which the cobalt center displays a local trigonal bipyramidal geometry (Fig. 1C).[12] The IR spectrum of a hexanes suspension of InP-$In[Co(CO)_4]_3$ NCs shows three ν_{CO} bands at 2075, 2013,

and 1986 cm^{-1}, also consistent with C_{3v}-symmetric $[Co(CO)_4]^-$ fragments coordinated to surface In^{3+} centers (Fig. 1D bottom). These bands exhibit higher frequencies compared to those of the CdSe-$Cd[Co(CO)_4]_2$ NCs, likely corresponding to the higher electronegativity and charge of In^{3+} compared to Cd^{2+}. Similar differences are observed for the ν_{CO} bands of the parent complexes $Cd[Co(CO)_4]_2$ (2084, 2021, and 2000 cm^{-1})[20] and $In[Co(CO)_4]_3$ (2092, 2069, and 2002 cm^{-1}).[21]

The IR spectrum for InP-$In[Co(CO)_4]_3$ NCs also shows other smaller bands in the ν_{CO} region. While we have not positively identified these species, these additional bands may arise from different populations of $[Co(CO)_4]^-$ anions at different surface In^{3+} sites, as InP NCs are tetrahedra and so exhibit facet and edge sites compared to the spheroidal CdSe NCs (Fig. S10).[15] Additionally, it is possible that the functionalized surface In^{3+} sites could be coordinated by 1, 2, or 3 $[Co(CO)_4]^-$ anions, with the remaining positive charge compensated by chloride anions. We similarly cannot entirely rule out mixed-ligand $Cd(OA)[Co(CO)_4]$ sites at CdSe NC surfaces, but have observed experimental evidence so far for only $Cd[Co(CO)_4]_2$ species (see below).

Ligand displacement reactions

Addition of Lewis bases to samples of CdSe-$Cd[Co(CO)_4]_2$ NC samples results in L-type-assisted Z-type displacement of the $Cd[Co(CO)_4]_2$ moiety in the form of the Lewis base adduct of the cadmium cobaltate compound, $L_nCd[Co(CO)_4]_2$ (Eq. 1, L = THF, pyridine, TMEDA, n = 1–2). Equation 2 shows the analogous L-type-assisted Z-type displacement of $Cd(OA)_2$ from the same NC sample.

$$\text{CdSe-}Cd[Co(CO)_4]_2 + n\ L \rightleftharpoons CdSe + L_nCd[Co(CO)_4]_2 \quad (1)$$

$$\text{CdSe-}Cd(OA)_2 + n\ L \rightleftharpoons CdSe + L_nCd(OA)_2 \quad (2)$$

These two Z-type ligand displacement reactions are expected to exhibit different equilibrium constants due to both electronic and steric differences between the $Cd[Co(CO)_4]_2$ and $Cd(OA)_2$ ligands.

Figure 2 shows the IR spectra of hexanes suspensions of CdSe-$Cd[Co(CO)_4]_2$ NCs (0.7 mM) with increasing concentrations of added THF (7 mM – 12.3 M, 10–18,000 equiv/NC). In these spectra, the three ν_{CO} bands of the surface-bound $[Co(CO)_4]^-$ moiety shift to lower energies with increasing [THF] and new, sharper ν_{CO} bands grow that match those of $(THF)_nCd[Co(CO)_4]_2$ independently prepared by treatment of $Cd(OAc)_2$ with $Et_3SiCo(CO)_4$. Purification by GPC results in isolation of NC samples with no ν_{CO} bands in the IR spectrum, indicating that this new carbonyl-containing fragment is not coordinated to the NC surface. Scheme 3 diagrams this proposed THF-mediated Z-type ligand displacement.

$(THF)_nCd(OA)_2$ is not displaced under the same conditions. ^{1}H NMR spectroscopy of a C_6D_6 suspension of CdSe-$Cd[Co(CO)_4]_2$ NCs (100 OA^-/NC) with added THF (25 – 240 equiv/NC) shows only broadening and a slight upfield shift of the OA^--derived alkenyl ^{1}H resonance at 5.65 ppm, but no sharp peak corresponding to the molecular species $(THF)_nCd(OA)_2$ (Fig. S15B). For example, the alkenyl protons of a related molecular $(TMEDA)Cd(OA)_2$ species have previously been reported to display a ^{1}H NMR resonance at 5.49 ppm in C_6D_6 solution.[1] Displacement of a putative mixed-ligand $(THF)_nCd(OA)[Co(CO)_4]$ species would also be expected to result in a sharp ^{1}H NMR resonance, but this is also not observed. IR spectroscopy of the same mixtures shows a decrease in the ν_{CO} band intensities of the NC-bound $[Co(CO)_4]^-$ of up to 90%, corresponding to displacement of ca. 10 $Cd[Co(CO)_4]_2$ NC^{-1}. Taken together, these data show that $Cd[Co(CO)_4]_2$ Z-type ligands are more readily displaced by THF than $Cd(OA)_2$.

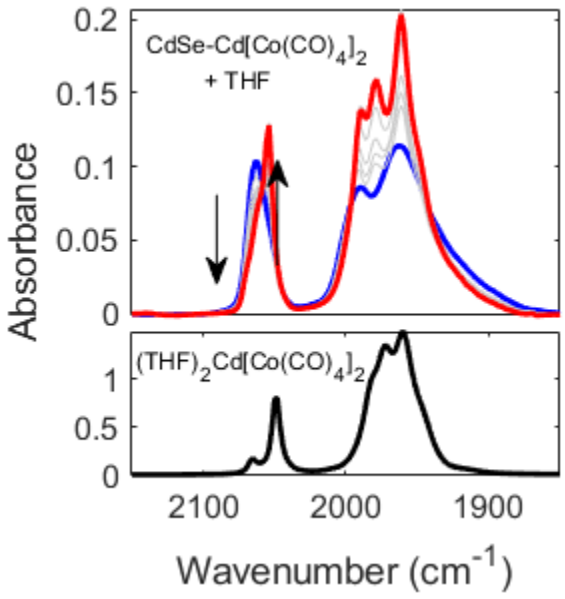

Figure 2. IR spectra of a hexanes suspension of CdSe-$Cd[Co(CO)_4]_2$ NCs (d ~ 3.8 nm, 0.7 mM, blue) with increasing concentrations of THF (7 mM–12.3 M). The red line is the spectrum taken with [THF] = 12.3 M, and matches the IR spectrum of a THF solution of $(THF)_2Cd[Co(CO)_4]_2$ independently prepared by treatment of $Cd(OAc)_2$ with $Et_3SiCo(CO)_4$ in the absence of CdSe NCs.

Scheme 3. L-type ligands displace Z-type $Cd[Co(CO)_4]_2$ from CdSe-$Cd[Co(CO)_4]_2$ NC surfaces. When L = Me_3NO, the displaced $L_2Cd[Co(CO)_4]_2$ complex undergoes further ionic dissociation.

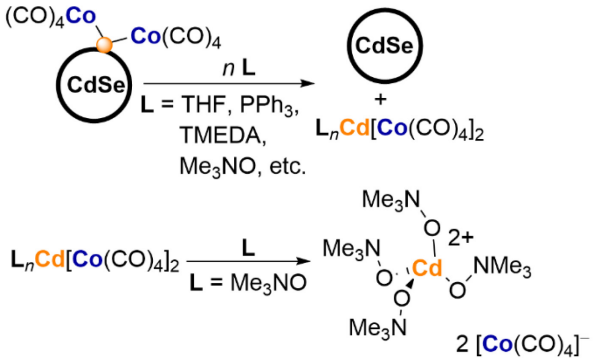

The addition of nitrogen donors like pyridine or TMEDA also displaced the corresponding $L_nCd[Co(CO)_4]_2$ compounds (L = pyridine, TMEDA, n = 2 or 1 respectively) from CdSe-

$Cd[Co(CO)_4]_2$ NCs, as measured by IR spectroscopy (Fig. S16, S17). In the latter case, displacement of $(TMEDA)Cd(OA)_2$ was also observed by ^1H NMR spectroscopy (Fig. S17A, S18). Although the Z-type coordination of $Cd(OA)_2$ have been previously demonstrated to follow a two-site binding isotherm,[7-8] here the equilibrium constants of $Cd[Co(CO)_4]_2$ and $Cd(OA)_2$ displacement were compared based on a simplified one-site binding model using the reactions shown in equations 1 and 2, where $K_{eq} = \frac{[TMEDACdX_2][CdSe\text{-}B]}{[CdSe\text{-}B{:}CdX_2][TMEDA]}$, B is a NC surface binding site for a Z-type ligand, and X^- = OA^- or $[Co(CO)_4]^-$. For the displacement of $Cd(OA)_2$ from these samples, the equilibrium constant is estimated to be about 0.02, which is consistent with previously reported values.[7] The equilibrium constant for displacement of $Cd[Co(CO)_4]_2$ is approximately 2, meaning that variation of the anion coordinated to Cd^{2+} can change the thermodynamics of Z-type ligand displacement of CdX_2 species from NC surfaces.

When phosphines and phosphite ligands (PR_3, R = Et, Ph, OPh, OMe) were added to CdSe-$Cd[Co(CO)_4]_2$ NCs, initial Z-type displacement of $Cd[Co(CO)_4]_2$ was followed by substitution of carbonyl for the corresponding phosphine or phosphite. For example, GPC purification of a mixture of CdSe-$Cd[Co(CO)_4]_2$ NCs treated with PPh_3 (200 equiv/NC) resulted in isolation of CdSe NCs with no coordinated cobalt along with molecular $(THF)_2Cd[Co(CO)_3PPh_3]_2$, which was confirmed by comparison of the IR spectra to reported complexes (Fig. S20-S22).[22]

The addition of trimethylamine *N*-oxide (Me_3NO) or pyridine *N*-oxide to CdSe-$Cd[Co(CO)_4]_2$ NCs resulted in different ligand displacement reactions. The IR spectra of a toluene suspension of CdSe-$Cd[Co(CO)_4]_2$ NCs with increasing addition of Me_3NO (10–200 equiv/NC) show conversion of the CdSe-$Cd[Co(CO)_4]_2$ NCs first to a new $[Co(CO)_4]^-$-containing species assigned as $(Me_3NO)_nCd[Co(CO)_4]_2$ (L-type-assisted Z-type ligand displacement, Fig. S23). Further addition of Me_3NO to the mixture results in consumption of this species and growth of a single,

lower energy ν_{CO} band at 1886 cm^{-1}. This new band is consistent with the IR spectrum of dissociated tetracarbonylcobaltate anion, $[Co(CO)_4]^-$.[23-24] The remaining counter-cation is likely the dicationic $[(Me_3NO)_4Cd]^{2+}$ species (Scheme 3).[25] Addition of pyridine N-oxide (pyO) or triphenylphosphine oxide to CdSe-$Cd[Co(CO)_4]_2$ NCs results in similar IR spectra (Fig. S24, S25). As a control experiment, addition of Me_3NO to $(THF)_2Cd[Co(CO)_4]_2$ in the absence of CdSe NCs also forms the same product by IR spectroscopy (Fig. S26). While we have been unable to grow X-ray-quality single crystals of this salt, molecular metal tetracarbonylcobaltate compounds have previously been reported to undergo similar ionic dissociation in *N*,*N*-dimethylformamide solution.[26] Related $(pyO)_2CdX_2$ and $[(pyO)_6Cd][CdX_4]$ species have also been reported to form upon addition of pyO to cadmium halides.[27-29] These differences could be related to the relative "donicity" of the Lewis bases, which has been previously quantified by a donor number (DN) value that is related to the enthalpic change upon forming a 1:1 adduct with $SbCl_5$. For example, THF is a moderate Lewis base, with DN ~ 20 kcal/mol, while octylamine *N*-oxide molecule has been reported to have a DN of 52 kcal/mol.[30]

Next, we compared displacement of the Z-type ligand $In[Co(CO)_4]_3$ from InP NC surfaces to the displacement reactions of $Cd[Co(CO)_4]_2$ from CdSe NC surfaces discussed above. The IR spectrum of a toluene suspension of InP-$In[Co(CO)_4]_3$ NCs with added THF does not show ν_{CO} band corresponding to free $In[Co(CO)_4]_3$, which are reported at 2076, 2069, and 2002 cm^{-1} in cyclohexane.[21] Instead, a single ν_{CO} band at 1886 cm^{-1} corresponding to the free anion $[Co(CO)_4]^-$ is observed (Fig. S27). GPC purification of the reaction mixture removes the free $[Co(CO)_4]^-$, indicating that this free anion is not associated with the NC itself, and ICP-OES of the purified NCs shows fewer Co atoms/NC (44 ± 0.2). ^1H NMR spectroscopy of the purified NC sample after THF-assisted $In[Co(CO)_4]_3$ displacement shows a decrease in the concentration of surface-bound

$OlNH_2$; these data are consistent with additional L-type ligand exchange between THF and surface-bound $OlNH_2$ ligands.

We propose that Z-type displacement of $In[Co(CO)_4]_3$ from the InP NC surface occurs first to form $(THF)In[Co(CO)_4]_3$ that then dissociates to form a charge-separated salt $[(THF)_mIn(Co(CO)_4]_2][Co(CO)_4]$. This latter species would be expected to display a ν_{CO} band at 1886 cm^{-1}, as observed, as well as higher energy ν_{CO} bands corresponding to $[Co(CO)_4]^-$ moieties coordinated to In. As the IR spectrum of InP-$In[Co(CO)_4]_3$ NCs in THF does not show any ν_{CO} bands that could correspond to $In[Co(CO)_4]_3$ species, this secondary anion dissociation may be fast. As a control experiment, in our hands a THF solution of independently-prepared $In[Co(CO)_4]_3$ also forms a similar charge-separated salt that displays IR signals corresponding to free $[Co(CO)_4]^-$ (Fig. S28).[21]

To compare whether this difference in Z-type displacement is due to differences between the Z-type ligands or differences between the semiconductor NC composition, the mixed-metal system was targeted. A toluene suspension of zinc blende CdSe-$Cd(OA)_2$ NCs (d ~ 4.0 nm) was treated with independently prepared $In[Co(CO)_4]_3$ to form "CdSe-$In[Co(CO)_4]_3$" NCs (Scheme 4A).[21] Figure 3 shows the IR spectrum of a toluene suspension of the NC sample after GPC purification. The ν_{CO} bands are shifted from those of the $In[Co(CO)_4]_3$ precursor, consistent with association to the NC surface. ICP-OES measurements of different batches of CdSe-$In[Co(CO)_4]_3$ NC samples showed a range of 9−10 In atoms/NC and 11−20 Co atoms/NC.

Scheme 4. (A) Addition of $In[Co(CO)_4]_3$ to CdSe-$Cd(OA)_2$ NCs results in anion exchange between the ligands of surface Cd^{2+} and In^{3+}. THF addition displaces $Cd[Co(CO)_4]_2$. (B) Addition of $Cd[Co(CO)_4]_2$ to InP NCs does not result in anion exchange between Cd^{2+} and In^{3+}. Addition of THF displaces $(THF)_2Cd[Co(CO)_4]_2$.

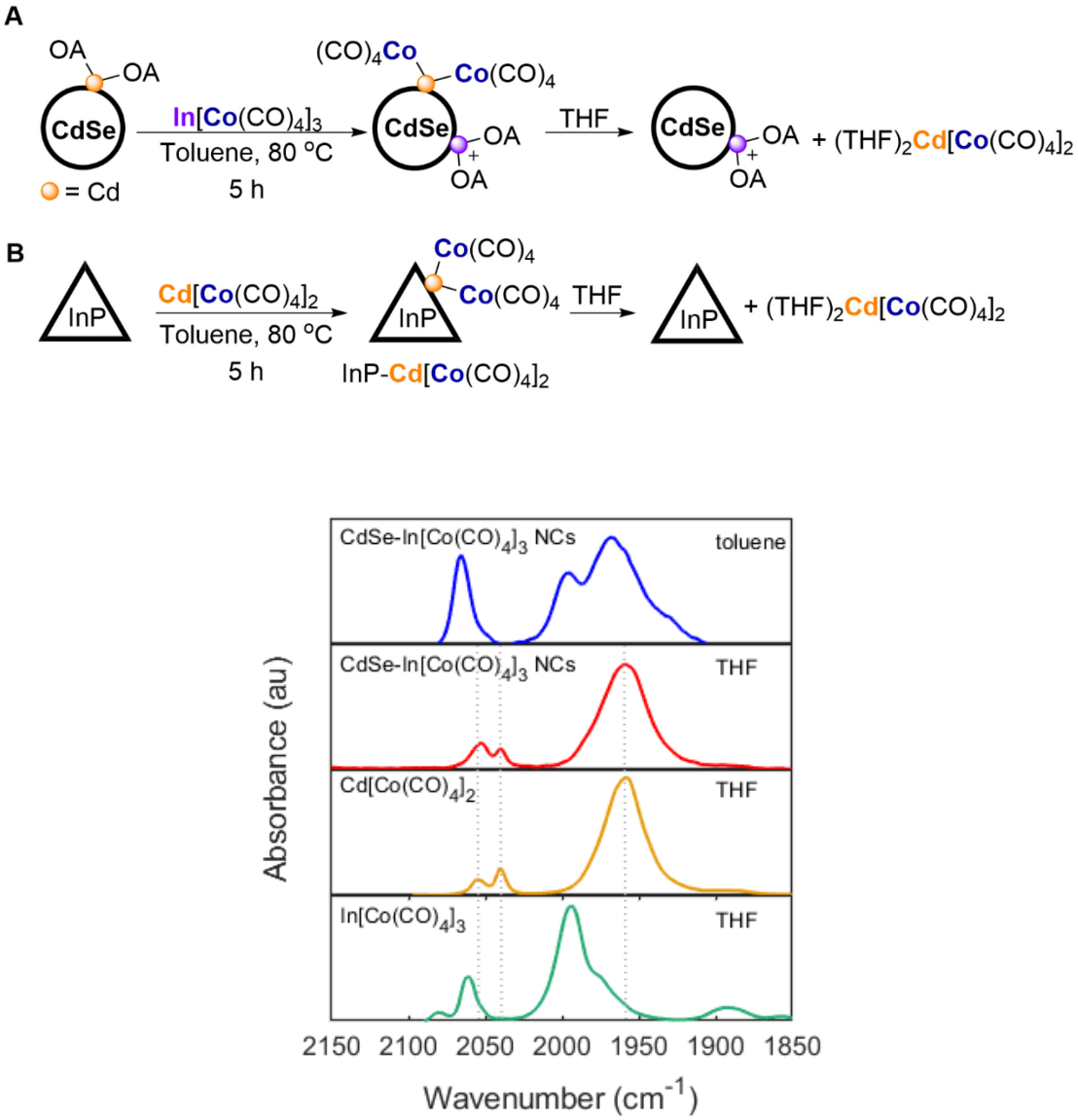

Figure 3. Comparison of the IR spectra of CdSe-In[Co(CO)$_4$]$_3$ NCs in toluene (blue) and in THF (red), showing displacement of Cd[Co(CO)$_4$]$_2$ in THF. IR spectra of THF solutions of independently-prepared Cd[Co(CO)$_4$]$_2$ (orange) and In[Co(CO)$_4$]$_3$ (green) are included for comparison, demonstrating that only Cd[Co(CO)$_4$]$_2$ is displaced from the NC surface. Dotted lines are shown as a guide to the eye.

Figure 3 also compares the IR spectrum of "CdSe-In[Co(CO)$_4$]$_3$" NCs suspended in THF with the IR spectra of THF solutions of independently prepared molecular Cd[Co(CO)$_4$]$_2$ and

$In[Co(CO)_4]_3$ species in the absence of NCs. The ν_{CO} bands of the NC suspension in THF are shifted to lower energies compared to the same suspension in toluene, consistent with THF-mediated displacement of a metal tetracarbonylcobaltate species. The IR spectrum of this displaced species matches that of $(THF)_2Cd[Co(CO)_4]_2$ and not $In[Co(CO)_4]_3$, indicating that THF displaces $Cd[Co(CO)_4]_2$ from the "CdSe-$In[Co(CO)_4]_3$" NC surfaces rather than $In[Co(CO)_4]_3$. The preferred association of $[Co(CO)_4]^-$ anions with surface Cd^{2+} centers indicates that X-type ligand exchange occurs between surface-bound $Cd(OA)_2$ and the added $In[Co(CO)_4]_3$. The resulting In^{3+} in the NC sample is most likely coordinated by OA^- ligands, but these surface-bound $In(OA)_3$ species cannot be distinguished by ^{1}H NMR spectroscopy. ^{1}H NMR quantification of the resulting NC sample also indicates lower surface OA^- concentrations (ca. 110 OA^-/NC), consistent with loss of some $In(OA)_3$ or $Cd(OA)_2$ during purification.

ICP-OES analysis of the GPC-purified NC sample obtained post THF treatment shows removal of Co atoms (4 Co atoms/NC remaining), but minimal removal of In atoms (9 In atoms/NC remaining). These data are also consistent with THF-mediated displacement of $Cd[Co(CO)_4]_2$ instead of $In[Co(CO)_4]_3$. As a control experiment to demonstrate that X-type ligand exchange between Cd^{2+} and In^{3+} is possible, a mixture of independently-prepared $Cd(OA)_2$ and $In[Co(CO)_4]_3$ in the absence of NCs also shows anion exchange by IR spectroscopy (Fig. S29).

These results were compared to the converse reaction. Treatment of a toluene suspension of InP NCs (l = 4.5 nm, 0.8 mM) with $Cd[Co(CO)_4]_2$ (25 equiv/NC) afforded "InP-$Cd[Co(CO)_4]_2$" NCs after GPC purification (Scheme 4B, 38 Co/NC). The ν_{CO} bands in the IR spectrum of this sample are broadened and shifted to higher energies compared to a toluene solution of independently prepared $Cd[Co(CO)_4]_2$, consistent with coordination to the InP NC surface (Fig. S30). Resuspension of this sample in THF leads to Z-type displacement of $(THF)_2Cd[Co(CO)_4]_2$ (IR

spectroscopy), with a decrease in surface-bound Co, as measured by ICP-OES analysis (Table S2). No displacement of $In[Co(CO)_4]_3$ was observed, meaning that X-type exchange between $Cd[Co(CO)_4]_2$ and the native surface In^{3+} species of the InP NCs did not occur.

Comparison of X-type Ligand Effects on Z-Type Binding.

Next, the effects of different anions on Z-type ligand binding to CdSe NCs rather than displacement were studied. Figure 4 shows the PL enhancement of benzene solutions of OA^--capped zinc blende CdSe NC samples (d ~ 3.7 nm, PLQY = 5%) upon addition of increasing amounts of cadmium carboxylate salts (carboxylate = OA^-, 3,5-ditertbutylbenzoate, and trifluoroacetate) added as THF solutions. These samples were allowed to mix at room temperature before the emission measurement but were not heated or otherwise treated with additional amine. Each of these samples undergo initial PL enhancement upon addition of the CdX_2 salts, but the maximum increase is achieved with fewer equivalents of $Cd(O_2CCF_3)$ (ca. 25 equiv/NC) compared to $Cd(OA)_2$ or $Cd(O_2CAr)_2$ (ca. 100 equiv/NC). CdX_2 salts with smaller anions like $CdCl_2$ or $Cd(OAc)_2$ were not studied due to their insolubility in the nonpolar organic solvents used here. Addition of $(THF)_2Cd[Co(CO)_4]_2$ to the CdSe NCs resulted in complete quenching of PL, and is not included in the plot.

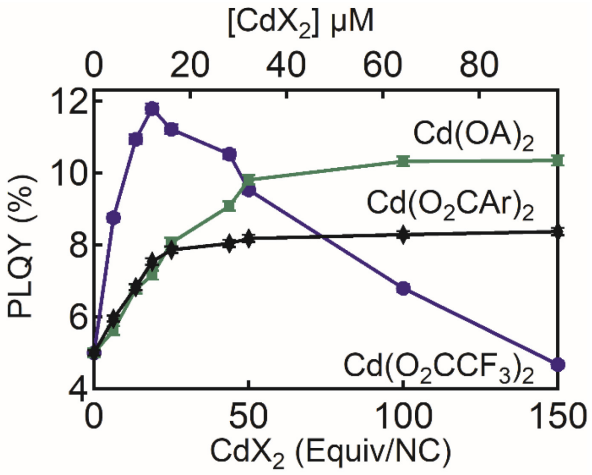

Figure 4. Relative increase in emission of benzene solutions of OA^--capped CdSe NCs (0.55 μM) with increasing concentrations of CdX_2 [X^- = OA^- (green); $^-O_2CCF_3$ (blue); 3,5-di-*tert*-butylbenzoate (^-O_2CAr, black)], added as THF solutions.

The PLQY dependence upon addition of $Cd(OA)_2$ and cadmium 3,5-di-*tert*-butylbenzoate reach a maximum value at ca. 60 μM of the added cadmium salts. In contrast, the PLQY of the CdSe NC samples treated with $Cd(O_2CCF_3)_2$ *decreases* with a large excess of $Cd(O_2CCF_3)_2$. Absorbance spectroscopy of this sample does not show NC precipitation or scattering. Samples prepared under N_2 in the glovebox in dry solvent also displayed the same PLQY behavior, indicating that H_2O or air are not involved. Although multiple NC surface factors could contribute to this quenching, one possible explanation is that the $Cd(O_2CCF_3)_2$ Z-type ligand is more readily displaced at higher THF concentrations (see below).**Anion effects on CdX_2 Lewis acidity**

To investigate possible explanations for differences in CdX_2 displacement or binding, the Lewis acidities of different CdX_2 salts (X^- = $Co(CO)_4^-$, $^-O_2CCF_3$, OA^-), $In[Co(CO)_4]_3$, and $B(C_6F_5)_3$ were compared using the Gutmann-Beckett method, which empirically relates Lewis acidity to the ^{31}P NMR shift of added Et_3PO.[31-32] Figure 5 shows the ^{31}P NMR spectra of CH_2Cl_2 solutions of Et_3PO upon addition of 1 equivalent of each corresponding CdX_2 salt or of $B(C_6F_5)_3$ as a standard. In these experiments, the ^{31}P NMR resonance shifts downfield from that of Et_3PO (δ 51.2 ppm) upon coordination of Et_3PO to the Lewis acids, and this chemical shift was converted into an empirical acceptor number value (AN) as a measure of Lewis acidity, where $AN = 2.21(\delta_{sample} - 41)$. Table 1 compares the chemical shifts and the AN values for the different CdX_2 salts studied here. From these experiments, it is apparent that the Lewis acidities of CdX_2 salts increase in the order $Cd(OA)_2 < Cd[Co(CO)_4]_2 < Cd(O_2CCF_3)_2$. This estimated Lewis acidity is likely a weighted average of a mixture of species. Blakemore and co-workers have demonstrated through binding

isotherm measurements that different numbers of phosphine oxide molecules can coordinate to different metal cations, with charge-dependent cooperative binding.[33-34]

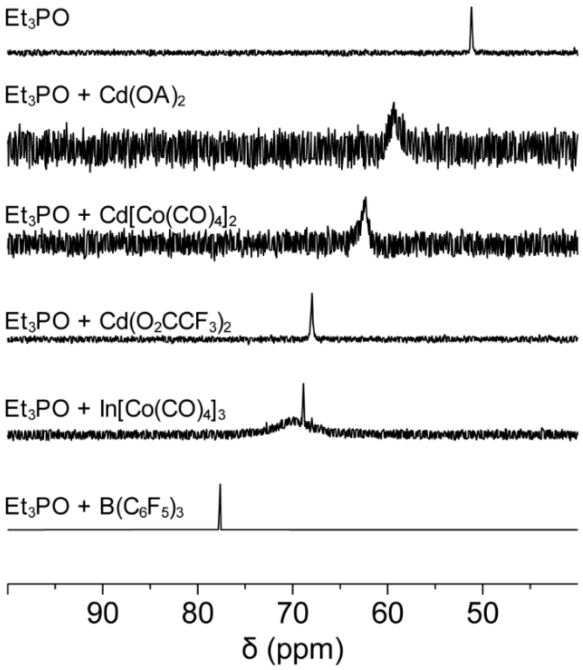

Figure 5. ^{31}P NMR spectra of CH_2Cl_2 solutions of Et_3PO (top) or of Et_3PO with added Lewis acid (1 equiv). Spectra are referenced against an external standard of 85% H_3PO_4.

Table 1. ^{31}P NMR chemical shifts for 1:1 mixtures of Et_3PO and Lewis acid in CH_2Cl_2 and calculated AN values.

Lewis Acid	$\delta(^{31}P)$	AN
none	51.2	22.5
$Cd(OA)_2$	59.3	40.4
$Cd[Co(CO)_4]_2$	62.5	47.5
$Cd(O_2CCF_3)_2$	68	60.0

$In[Co(CO)_4]_3$[a]	69.7	63.4
$B(C_6F_5)_3$	77.6	80.9

[a]$\delta(^{31}P)$ and AN were determined from the weighted average of the observed resonances.

These experiments demonstrate that the Lewis acidity of the cadmium center of CdX_2 species depends on the electronics of the coordinated anion. As expected, more electron-rich anions like OA^- result in less Lewis acidic CdX_2 species. A complication of this analysis is that the coordination of X-type ligands may vary. While the $[Co(CO)_3L]^-$ anions (L = CO, PR_3) exhibit terminal, monodentate coordination to Cd^{2+} centers, ligands like carboxylate can exhibit monodentate, chelating bidentate, and bridging coordination modes. These bridging motifs can lead to dynamically exchanging cluster formation from the CdX_2 complexes in solution upon displacement, complicating the Lewis acidity analysis. For these reasons, the measured Gutmann-Beckett acidity value for these species may in fact be a weighted average of multiple cadmium carboxylate species. Nevertheless, these values should be good approximations of overall Lewis acidity.

To compare the influence of the metal, the ^{31}P NMR spectrum of a mixture of Et_3PO and $In[Co(CO)_4]_3$ was also measured (Fig. 5). The spectrum shows multiple ^{31}P NMR resonances that may arise from different coordination numbers of Et_3PO around In; the AN was then calculated from the weighted average of these values (Table 1). The higher Lewis acidity of $In[Co(CO)_4]_3$ (AN = 63.4) compared to the cadmium congener $Cd[Co(CO)_4]_2$ (AN = 47.5) is also consistent with the trends predicted when using the pK_a's of the metal aqua species as a proxy for Lewis acidity (pK_a ~ 4.43 for In^{3+} and 10.2 for Cd^{2+}).[35]

DISCUSSION

Anion effects on Z-type ligand coordination to NC surfaces

The experiments above demonstrated that the more Lewis acidic $Cd[Co(CO)_4]_2$ species was more readily displaced than $Cd(OA)_2$ from CdSe NC surfaces by Lewis basic donors (THF, phosphines, TMEDA, Me_3NO, etc.). Although stronger Lewis acids might be expected to act as better Z-type ligands, the equilibrium constants of L-type-assisted Z-type ligand displacement reactions are dictated by the overall stability of the displaced molecular L_nCdX_2 product compared to the NC-bound CdX_2 species. When the X-type ligand is more basic (e.g., $X^- = OA^-$), the less Lewis acidic Z-type CdX_2 ligand is less likely to undergo displacement from the NC surface in coordinating solvents because the Lewis adduct formed upon coordinated the Lewis base L, L_nCdX_2, is less stabilized. In short, the NC surface itself is not a strong Lewis base compared to THF or other donors.

This result has implications for ligand surface passivation of NC samples. Metal halide salts have been used to improve the PLQY of CdSe, CdTe, and InP NCs.[3, 17, 36] However, halide anions are less electron-donating compared to carboxylate ligands due to their greater electronegativity. The corresponding CdX_2 ($X^- = Cl^-$, Br^-, and I^-) salts would be expected to be more Lewis acidic compared to $Cd(OA)_2$, but might then be more readily displaced in the presence of donating solvents or other Lewis bases. Further, some procedures for introducing Z-type ligands to NC samples involve heating in amine solutions, which might be expected to change the speciation of the metal salts themselves, for example to form charge-separated ion pairs such as $[(amine)_nCd]X_2$ species.

Metal effects on Z-type ligands

The experiments above also showed that, despite the higher covalency of InP compared to CdSe,[37] both NC samples exhibit similar Z-type ligand displacement and coordination reactions, consistent with previous reports. However, the results above also demonstrate that the CdX_2 and

InX_3 salts themselves behave differently from each other. First, $Cd[Co(CO)_4]_2$ was demonstrated to be less Lewis acidic compared to $In[Co(CO)_4]_3$ based on the Gutmann-Beckett measurement. This trend likely extends to other CdX_2 and InX_3 salts. Second, the observation that addition of $In[Co(CO)_4]_3$ to CdSe-$Cd(OA)_2$ NCs results in the formation of surface-bound $Cd[Co(CO)_4]_2$ species shows that anion exchange between In^{3+} and Cd^{2+} is facile and driven by the relative energies of Cd–Co, In–Co, Cd–O, and In–O bonds. Both of these factors contribute to the observation that $In[Co(CO)_4]_3$ undergoes ionic dissociation in THF solution, while $Cd[Co(CO)_4]_2$ does not.

This metal-dependent behavior likely affects experiments in which different metal salts are added as Z-type ligands to increase PLQY in NC samples.[3-4] For example, Dempsey and co-workers have recently compared the coordination of cadmium, zinc, and lead carboxylates to CdSe NCs, and observed metal-dependent PLQY increases attributed to the relative reduction potentials of the metal cation.[4] When metal salts (e.g. metal halides) with different counter-anions than the native NC ligands are added as Z-type ligands, however, an increase in PL may indicate Z-type passivation by the added metal salt but may also indicate changes to NC surface binding of *existing* surface cations upon X-type exchange. These processes would be dependent on the relative stabilities of the respective metal–anion bonds to drive the example exchange reaction shown in Equation 3, where MCl_2 is the chloride salt of a divalent metal added as a Z-type ligand to CdSe NCs.

$$\text{CdSe-Cd(OA)}_2 + MCl_2 \rightleftharpoons \text{CdSe-CdCl}_2 + M(OA)_2 \qquad (3)$$

The equilibrium constant of the above reaction is difficult to measure, as discussed above, but might be approximated by comparison of the respective M–O and M–Cl bond dissociation energies (BDEs). A similar approach has been used to quantify the empirical concepts of oxophilicity and thiophilicity.[38] Table 2 compares the BDEs of selected M–O and M–Cl bonds (D_O and D_{Cl},

respectively), as well as $\Delta D_{\mathrm{OCl}} = D_{\mathrm{O}} - D_{\mathrm{Cl}}$. These values suggest that Zn and Cd may be coordinated by carboxylate and halide anions with similar energies, but that Hg, Pb, and In may show marked preferences for ligand type, potentially resulting in anion exchange upon addition of their salts to NCs with different native cations. As these BDE values of gaseous diatomic molecules are admittedly inaccurate estimates of solution-phase, two-electron ligand exchange processes, experimental studies to test this hypothesis are ongoing.

Table 2. Experimental BDEs (kcal/mol) of diatomic molecules from reference 35.[39]

Metal	D_{O} (M)	D_{Cl} (M)	ΔD_{OCl}(M)
Zn	≤60	54.5	ca. 5.5
Cd	56.4	49.8	6.6
Hg	64.3	22.0	42.3
Pb	91.4	71.9	19.5
In	82.8	104.2	-21.4

CONCLUSIONS

We have demonstrated that $[Co(CO)_4]^-$ can be added to CdSe and InP NC surfaces as an X-type ligand. IR spectroscopy of these samples permits interrogation of ligand coordination equilibria. The X-type ligand tunes the equilibria of L-type-assisted Z-type displacement from NC surfaces. More electron-rich X-type ligands form CdX_2 Z-type ligands that are less Lewis acidic but also less readily displaced by coordinating solvents or by added Lewis bases (e.g. amines, phosphines). For example, the addition of THF displaces only the more Lewis acidic $Cd[Co(CO)_4]_2$ ligand, although stronger Lewis bases like TMEDA displace both $Cd[Co(CO)_4]_2$ and $Cd(OA)_2$. Beyond

$[Co(CO)_4]^-$-functionalized NCs, cadmium carboxylate salts show carboxylate-dependent effects on PLQY enhancement. These results suggest that anion exchange strategies could be valuable for tuning the stability of NC surfaces toward hole trap passivation.

EXPERIMENTAL SECTION

General Considerations. Unless otherwise indicated, all procedures were carried out in oven-dried glassware in an MBraun glovebox under an atmosphere of purified nitrogen or using a Schlenk line. Benzene-d_6 was purchased from Cambridge Isotope Laboratories, dried over sodium benzophenone ketyl radical, and distilled by vacuum transfer. Anhydrous THF, CH_3CN, diethyl ether, CH_2Cl_2, and hexanes were purified using the Grubbs method on a J.C. Meyer solvent system.[40]

Unless otherwise stated, the following commercial chemicals were used without further purification. 1-Octadecene (ODE) was purchased from Acros Organics. HOA, cadmium oxide, selenium dioxide, Me_3NO and PPh_3, PBu_3, $P(OPh)_3$, $P(OEt)_3$, and $P(OMe)_3$ were purchased from Sigma-Aldrich. Dicobalt octacarbonyl was purchased from Strem. Triethylsilane was purchased from Oakwood Chemicals. H_2O_2 and HNO_3 used for ICP-OES measurements were of AR Select (ACS) grade for trace metal determination. *N,N,N′,N′*-tetramethylethylenediamine (TMEDA) was dried over CaH_2 and distilled under vacuum. Anhydrous $CdCl_2$, $Cd(OAc)_2$, and $InCl_3$ were prepared by heating at 110 °C under vacuum for 18 h. Celite was dried under vacuum at 300 °C for 3 days. $Na[Co(CO)_4]$, $Et_3SiCo(CO)_4$, $[Co(CO)_3PR_3]_2$, (R = Ph, Bu, OPh, and OMe), and $In[Co(CO)_4]_3$ were synthesized following reported procedures.[1-5] $Et_3SiCo(CO)_4$ was synthesized following reported procedures and purified via vacuum distillation prior to use.[41] Zinc blende CdSe and InP NCs were synthesized using Schlenk line techniques under dinitrogen following published

procedures (see SI for details).[15, 42-44] NC sizes and concentrations were determined optically.[15, 45-46]

Caution! Cadmium is toxic and should be handled with care.

Sample Characterization. Absorption spectra were collected on an Agilent Cary 60 spectrophotometer, using sealable 1-cm-path-length quartz cuvettes. ^{1}H NMR spectra were collected on a Bruker 400 MHz or Bruker 500 MHz instrument, with chemical shifts reported relative to the residual solvent peak (δ 7.16 ppm for benzene-d_6). ^{1}H NMR spectra of NC samples were collected using eight scans with a 30 s relaxation delay. ^{31}P NMR spectra were reported relative to an external standard of 85% H_3PO_4 (δ 0.0 ppm) with a d1 time of 2 s. FTIR spectra were collected in THF, toluene, hexanes, or CH_2Cl_2 solution samples in demountable Pike liquid cell with CaF_2 or KBr windows and a path length of 0.25 mm, using a Nicolet 380 FT/IR spectrometer. PXRD data were collected on samples drop cast onto a glass slide, using a Bruker AXS D8 Advance diffractometer at a step rate of 0.2° from a 2θ value of 10−60°. Transmission electron microscopy (TEM) images were obtained on a Thermo Scientific™ Talos F200i microscope operating at 200 kV. Colloidal suspensions of the NC samples were drop cast onto a copper grid (Ultrathin Carbon Type-A, 400 mesh, Ted Pella) and dried under vacuum for 3 days inside the glovebox prior to analysis. Size distributions were determined by analysis of >200 individual NCs.

Synthesis of CdSe-Cd[Co(CO)$_4$]$_2$ NCs. In a representative procedure, in the glovebox, an oven-dried 50 mL Schlenk tube equipped with a stir bar was charged with a toluene suspension of CdSe-$Cd(OA)_2$ NCs (d ~ 4.0 nm, 1.3 mM, 10 mL, 0.013 mmol, 1 equiv). $Et_3SiCo(CO)_4$ (0.186 g, 0.65 mmol, 50 equiv/NC) was added. The reaction mixture was stirred at 80 °C under N_2 for 20 h, then cooled to room temperature. In the glovebox, the reaction mixture was purified by GPC to remove molecular byproducts.

Synthesis of InP-In[Co(CO)$_4$]$_3$ NCs. In the glovebox, an oven-dried Schlenk tube equipped with a stir bar was charged with a toluene suspension of InP NCs (l ~ 4.5 nm, 1.4 mM, 140 μmol, 10 mL). A toluene solution of $Et_3SiCo(CO)_4$ (1 M, 700 μmol, 50 equiv, 700 μL) was added and the tube was sealed with a Teflon stopper. The solution was stirred at 80 °C for 3–5 h. The reaction mixture was brought back into the glovebox and purified by GPC.

Synthesis of CdSe-In[Co(CO)$_4$]$_3$ NCs. In the glovebox, an oven-dried Schlenk tube equipped with a stir bar was charged with a toluene suspension of CdSe-Cd(OA)$_2$ NCs (d ~ 4.0 nm, 2.3 mM, 2.3 μmol, 1 mL). A toluene solution of In[Co(CO)$_4$]$_3$ (0.5 M, 69 μmol, 30 equiv, 0.14 mL) was added and the tube was sealed with a Teflon stopper. The solution was stirred at 80 °C for 5 h. The reaction mixture was brought back into the glovebox and purified by GPC.

Procedure for GPC Purification. Sample purification by GPC technique leaves the absorption features of NC samples unchanged, with no etching or aggregation observed.[14] To prepare the column, Bio-Beads SX-1 (BioRad Laboratories, 200−400 mesh, 4 g) were dried under vacuum at room temperature for 3 d. The beads were brought into the glovebox and stored in toluene for 12 h. The beads were transferred into a column (d ~ 2 cm) and flushed twice to remove any residual contaminants. The unpurified NC sample (ca. 1 mL in toluene, ca. 0.3 mM) was loaded onto the column and eluted with toluene using gravity. The first red band to elute was collected and dried under vacuum.

Quantification of OA$^-$ Concentration by ^{1}H NMR Spectroscopy. In the glovebox, a NC sample (ca. 0.6 μmol) was dried under vacuum and redissolved in a stock solution of 1,3,5-trimethoxybenzene in C_6D_6 (0.05 M, 0.5 mL). ^{1}H NMR spectra were collected using 10 scans with a 30 s relaxation delay. 10 μL of the NMR sample solution was diluted with toluene (3 mL), and a UV-vis absorption spectrum was measured to calculate the NC concentration.

Inductively Coupled Plasma Optical Emission Spectrometry (ICP-OES). ICP-OES samples were digested following a published procedure.[47] Briefly, a sample of CdSe-Cd[$Co(CO)_4$]$_2$ NCs (ca. 0.012 μmol) was dried under vacuum. 30% hydrogen peroxide solution (0.5 mL) was added to the residue and allowed to digest for 5 min. Concentrated HNO_3 was then added, and the solution was allowed to digest for 45 min. The sample was then passed through a syringe filter and diluted to 10 mL with 1% HNO_3 solution. ICP-OES data were collected on a PerkinElmer Optima 8000 in axial view.

Phosphine-Induced Displacement of Cd[$Co(CO)_4$]$_2$ from CdSe-Cd[$Co(CO)_4$]$_2$ NCs. In a representative procedure, in the glovebox, a scintillation vial equipped with a stir bar was charged with a toluene suspension of CdSe-Cd[$Co(CO)_4$]$_2$ NCs (0.8 mM, 2.5 mL, 0.002 mmol) and PPh_3 (0.03 g, 0.100 mmol, 50 equiv/NC). The reaction mixture stirred at room temperature for 20 h, during which a pale-yellow precipitate formed. The pale-yellow precipitate was isolated by filtration and washed with hexanes, then recrystallized from THF/hexanes to yield $(THF)_2Cd[Co(CO)_3PPh_3]_2$. The CdSe NC fraction was purified by GPC and analyzed by FTIR spectroscopy to confirm the absence of remaining surface-bound cobaltate.

THF-Induced Displacement of Cd[$Co(CO)_4$]$_2$ from CdSe-Cd[$Co(CO)_4$]$_2$ NCs. In the glovebox, a 4 mL scintillation vial was charged with CdSe-Cd[$Co(CO)_4$]$_2$ NCs (0.14 μmol) and dried under vacuum. Hexanes (0.189 mL) and THF (123 mM, 11 μL, 1.4 mmol, 10 equiv/NC) was added to the vial, and the mixture was allowed to react for 15 min. The reaction mixture was injected into an IR cell and the FTIR spectrum was collected. This procedure was repeated for different THF concentrations (20, 50, 100, 200, and 1000 equiv/NC) while maintaining the same total volume (0.2 mL).

Comparison of $LCd[Co(CO)_4]_2$ and $LCd(OA)_2$ dissociation equilibria (L = TMEDA). A toluene suspension of CdSe-$Cd[Co(CO)]_2$ NCs (d ~ 3.8 nm, 0.52 mM, 0.26 μmol) was dried under vacuum, resuspended in 0.5 mL C_6D_6, and transferred into an NMR tube. TMEDA (10 equiv, 2.6 μmol) was added to the tube and ^{1}H NMR spectrum immediately measured. The reaction was injected into an IR cell for FTIR measurement. This procedure was repeated for different TMEDA concentrations (20, 30, and 128 equiv/NC).

Addition of Me_3NO to CdSe-$Cd[Co(CO)_4]_2$ NCs. In the glovebox, a scintillation vial equipped with a stir bar was charged with Me_3NO (0.009 g, 0.12 mmol, 200 equiv/NC). A toluene suspension of CdSe-$Cd[Co(CO)_4]_2$ NCs (0.6 mM, 0.6 μmol, 1 mL) was added, and the reaction mixture was stirred at room temperature for 1 h before IR measurement.

Gutmann acceptor number (AN) measurement. In the glovebox, a stock solution of $Et_3P{=}O$ in CH_2Cl_2 (0.6 mL, 50 mM, 0.03 mmol) was added to a scintillation vial charged with the corresponding Lewis acid (0.03 mmol, 1 equiv). The resulting solution was transferred to a NMR tube and measured by ^{31}P NMR spectroscopy.

Cadmium carboxylate addition to CdSe NCs. Under N_2, a 1-cm quartz cuvette was charged with a benzene solution of CdSe-$Cd(OA)_2$ NCs (d ~3.6 nm, 4 mL, 0.55 μM). In separate scintillation vials, stock solution of CdX_2 ($X^- = {}^-O_2CCF_3$, OA^-, and ^-O_2CAr, Ar = 3,5-di-*tert*-butylphenyl), were prepared in THF (1.38 mM). These solutions were incrementally added to the NC solution for the PL measurements.

PL Measurements. PL emission intensity was measured using an Ocean Optics USB2000+ spectrometer with 405 nm excitation. PLQY of the as-prepared CdSe-$Cd(OA)_2$ NCs (PLQY ~ 5%) was measured using an integrating sphere at an excitation wavelength of 370 nm, and the emission

measurements of other samples relative to the that of the CdSe-$Cd(OA)_2$ NCs were used to calculate their PLQY.

ASSOCIATED CONTENT

Supporting Information. Additional synthetic procedures. ^{1}H NMR spectra, IR spectra, electronic absorption spectra, and TEM images of samples and reaction mixtures.

AUTHOR INFORMATION

Corresponding Author

*Email: etsui@nd.edu

Author Contributions

The manuscript was written through contributions of all authors. All authors have given approval to the final version of the manuscript.

ACKNOWLEDGMENT

This work was supported by the NSF (CHE-2154948). ICP-OES measurements were conducted at the Center for Environmental Science and Technology (CEST) at the University of Notre Dame. We thank Jeffrey DuBose and Prashant Kamat for the use of fluorescence instrumentation in PLQY measurements. We also thank Alex Sheardy for assistance with TEM.

REFERENCES

1. Anderson, N. C.; Hendricks, M. P.; Choi, J. J.; Owen, J. S. Ligand Exchange and the Stoichiometry of Metal Chalcogenide Nanocrystals: Spectroscopic Observation of Facile Metal-Carboxylate Displacement and Binding. *J. Am. Chem. Soc.* **2013,** *135*, 18536-18548.
2. Jasieniak, J.; Mulvaney, P. From Cd-Rich to Se-Rich − the Manipulation of CdSe Nanocrystal Surface Stoichiometry. *J. Am. Chem. Soc.* **2007,** *129*, 2841-2848.
3. Kirkwood, N.; Monchen, J. O. V.; Crisp, R. W.; Grimaldi, G.; Bergstein, H. A. C.; du Fossé, I.; van der Stam, W.; Infante, I.; Houtepen, A. J. Finding and Fixing Traps in II–VI and III–V Colloidal Quantum Dots: The Importance of Z-Type Ligand Passivation. *J. Am. Chem. Soc.* **2018,** *140*, 15712-15723.

4. Kelm, J. E.; Dempsey, J. L. Metal-Dictated Reactivity of Z-Type Ligands to Passivate Surface Defects on CdSe Nanocrystals. *J. Am. Chem. Soc.* **2024,** *146*, 5252-5262.
5. Green, M. L. H. A new approach to the formal classification of covalent compounds of the elements. *J. Organomet. Chem.* **1995,** *500*, 127-148.
6. Owen, J. The coordination chemistry of nanocrystal surfaces. *Science* **2015,** *347*, 615-616.
7. Saniepay, M.; Mi, C.; Liu, Z.; Abel, E. P.; Beaulac, R. Insights into the Structural Complexity of Colloidal CdSe Nanocrystal Surfaces: Correlating the Efficiency of Nonradiative Excited-State Processes to Specific Defects. *J. Am. Chem. Soc.* **2018,** *140*, 1725-1736.
8. Drijvers, E.; De Roo, J.; Martins, J. C.; Infante, I.; Hens, Z. Ligand Displacement Exposes Binding Site Heterogeneity on CdSe Nanocrystal Surfaces. *Chem. Mater.* **2018,** *30*, 1178-1186.
9. Hartley, C. L.; Dempsey, J. L. Electron-Promoted X-Type Ligand Displacement at CdSe Quantum Dot Surfaces. *Nano Lett.* **2019,** *19*, 1151-1157.
10. Kessler, M. L.; Dempsey, J. L. Mapping the Topology of PbS Nanocrystals through Displacement Isotherms of Surface-Bound Metal Oleate Complexes. *Chem. Mater.* **2020,** *32*, 2561-2571.
11. Schival, K. A.; Gipson, R. R.; Prather, K. V.; Tsui, E. Y. Photoinduced Surface Charging in Iron-Carbonyl-Functionalized Colloidal Semiconductor Nanocrystals. *Nano Lett.* **2019,** *19*, 7770-7774.
12. Prather, K. V.; Lee, S.; Tsui, E. Y. Metal-Carbonyl-Functionalized CdSe Nanocrystals: Synthesis, Surface Redox, and Infrared Intensities. *Inorg. Chem.* **2021,** *60*, 4269-4277.
13. Prather, K. V.; Stoffel, J. T.; Tsui, E. Y. Z-Type Ligand Coordination at Colloidal Semiconductor Nanocrystals Modifies Surface Electrostatics. *Chem. Mater.* **2022,** *34*, 3976-3984.
14. Shen, Y.; Gee, M. Y.; Tan, R.; Pellechia, P. J.; Greytak, A. B. Purification of Quantum Dots by Gel Permeation Chromatography and the Effect of Excess Ligands on Shell Growth and Ligand Exchange. *Chem. Mater.* **2013,** *25*, 2838-2848.
15. Kim, K.; Yoo, D.; Choi, H.; Tamang, S.; Ko, J.-H.; Kim, S.; Kim, Y.-H.; Jeong, S. Halide–Amine Co-Passivated Indium Phosphide Colloidal Quantum Dots in Tetrahedral Shape. *Angew. Chem. Int. Ed.* **2016,** *55*, 3714-3718.
16. Leemans, J.; Dümbgen, K. C.; Minjauw, M. M.; Zhao, Q.; Vantomme, A.; Infante, I.; Detavernier, C.; Hens, Z. Acid–Base Mediated Ligand Exchange on Near-Infrared Absorbing, Indium-Based III–V Colloidal Quantum Dots. *J. Am. Chem. Soc.* **2021,** *143*, 4290-4301.
17. Dümbgen, K. C.; Leemans, J.; De Roo, V.; Minjauw, M.; Detavernier, C.; Hens, Z. Surface Chemistry of InP Quantum Dots, Amine–Halide Co-Passivation, and Binding of Z-Type Ligands. *Chem. Mater.* **2023,** *35*, 1037-1046.
18. Lei, H.; Li, J.; Kong, X.; Wang, L.; Peng, X. Toward Surface Chemistry of Semiconductor Nanocrystals at an Atomic-Molecular Level. *Acc. Chem. Res.* **2023,** *56*, 1966-1977.
19. Click, S. M.; Rosenthal, S. J. Synthesis, Surface Chemistry, and Fluorescent Properties of InP Quantum Dots. *Chem. Mater.* **2023,** *35*, 822-836.
20. Shim, M.; Guyot-Sionnest, P. n-type colloidal semiconductor nanocrystals. *Nature* **2000,** *407*, 981-983.
21. Patmore, D. J.; Graham, W. A. G. Organometallic Compounds with Metal-Metal Bonds. III. Tetracarbonylcobalt Derivatives of Gallium, Indium, and Thallium. *Inorg. Chem.* **1966,** *5*, 1586-1590.
22. Hieber, W.; Breu, R. Über Die Reaktionsweisen des Kobaltcarbonyl-Quecksilbers und Anderer Metall-Kobaltcarbonyle. *Chem. Ber.* **1957,** *90*, 1259-1269.
23. Friedel, R. A.; Wender, I.; Shufler, S. L.; Sternberg, H. W. Spectra and Structures of Cobalt Carbonyls1. *J. Am. Chem. Soc.* **1955,** *77*, 3951-3958.
24. Edgell, W. F.; Huff, J.; Thomas, J.; Lehman, H.; Angell, C.; Asato, G. THE INFRARED SPECTRA OF METAL CARBONYLATE IONS. BONDING CONSIDERATIONS. *J. Am. Chem. Soc.* **1960,** *82*, 1254-1255.
25. Drago, R. S.; Donoghue, J. T.; Herlocker, D. W. Transition Metal Ion Complexes of Trimethylamine N-Oxide. *Inorg. Chem.* **1965,** *4*, 836-839.
26. Burlitch, J. M. Ionic dissociation of some compounds containing covalent metal-metal bonds. *J. Am. Chem. Soc.* **1969,** *91*, 4562-4563.

27. Nieuwenhuyzen, M.; Robinson, W. T.; Wilkins, C. J. Cadmium halide complexes with pyridine-N-oxide, and their crystal structures. *Polyhedron* **1991,** *10*, 2111-2121.
28. Reedijk, J. The ligand properties of pyridine-N-oxide. Extension and discussion. *Recl. Trav. Chim. Pays-Bas* **1969,** *88*, 499-512.
29. Kida, S. The Preparation of Trimethylamine Oxide Complexes and Some Infrared Studies. *Bull. Chem. Soc. Jpn.* **2006,** *36*, 712-717.
30. Cataldo, F. A revision of the Gutmann donor numbers of a series of phosphoramides including TEPA. *Eur. Chem. Bull.* **2015,** *4*, 92-97.
31. Mayer, U.; Gutmann, V.; Gerger, W. The acceptor number — A quantitative empirical parameter for the electrophilic properties of solvents. *Monatshefte für Chemie / Chemical Monthly* **1975,** *106*, 1235-1257.
32. Beckett, M. A.; Strickland, G. C.; Holland, J. R.; Sukumar Varma, K. A convenient n.m.r. method for the measurement of Lewis acidity at boron centres: correlation of reaction rates of Lewis acid initiated epoxide polymerizations with Lewis acidity. *Polymer* **1996,** *37*, 4629-4631.
33. Kumar, A.; Blakemore, J. D. On the Use of Aqueous Metal-Aqua pKa Values as a Descriptor of Lewis Acidity. *Inorg. Chem.* **2021,** *60*, 1107-1115.
34. Golwankar, R. R.; Curry, T. D., II; Paranjothi, C. J.; Blakemore, J. D. Molecular Influences on the Quantification of Lewis Acidity with Phosphine Oxide Probes. *Inorg. Chem.* **2023**.
35. Perrin, D. D., *Ionisation constants of inorganic acids and bases in aqueous solution*. Pergamon Press: New York, 1982.
36. Sun, H.; Buhro, W. E. Reversible Z-Type to L-Type Ligand Exchange on Zinc-Blende Cadmium Selenide Nanoplatelets. *Chem. Mater.* **2020,** *32*, 5814-5826.
37. Kim, Y.; Chang, J. H.; Choi, H.; Kim, Y.-H.; Bae, W. K.; Jeong, S. III–V colloidal nanocrystals: control of covalent surfaces. *Chem. Sci.* **2020,** *11*, 913-922.
38. Kepp, K. P. A Quantitative Scale of Oxophilicity and Thiophilicity. *Inorg. Chem.* **2016,** *55*, 9461-9470.
39. *CRC Handbook of Chemistry and Physics*. CRC Press: Boca Raton, FL, 2014.
40. Pangborn, A. B.; Giardello, M. A.; Grubbs, R. H.; Rosen, R. K.; Timmers, F. J. Safe and Convenient Procedure for Solvent Purification. *Organometallics* **1996,** *15*, 1518-1520.
41. Chalk, A. J.; Harrod, J. F. Homogeneous Catalysis. IV. Some Reactions of Silicon Hydrides in the Presence of Cobalt Carbonyls. *J. Am. Chem. Soc.* **1967,** *89*, 1640-1647.
42. Parvizian, M.; Bechter, J.; Huber, J.; Chettata, N.; De Roo, J. An Experimental Introduction to Colloidal Nanocrystals through InP and InP/ZnS Quantum Dots. *J. Chem. Ed.* **2023,** *100*, 1613-1620.
43. Chen, O.; Chen, X.; Yang, Y.; Lynch, J.; Wu, H.; Zhuang, J.; Cao, Y. C. Synthesis of Metal–Selenide Nanocrystals Using Selenium Dioxide as the Selenium Precursor. *Angew. Chem. Int. Ed.* **2008,** *47*, 8638-8641.
44. Hamachi, L. S.; Jen-La Plante, I.; Coryell, A. C.; De Roo, J.; Owen, J. S. Kinetic Control over CdS Nanocrystal Nucleation Using a Library of Thiocarbonates, Thiocarbamates, and Thioureas. *Chem. Mater.* **2017,** *29*, 8711-8719.
45. Karel Čapek, R.; Moreels, I.; Lambert, K.; De Muynck, D.; Zhao, Q.; Van Tomme, A.; Vanhaecke, F.; Hens, Z. Optical Properties of Zincblende Cadmium Selenide Quantum Dots. *J. Phys. Chem. C* **2010,** *114*, 6371-6376.
46. Yu, W. W.; Qu, L.; Guo, W.; Peng, X. Experimental Determination of the Extinction Coefficient of CdTe, CdSe, and CdS Nanocrystals. *Chem. Mater.* **2003,** *15*, 2854-2860.
47. Morrison, C.; Sun, H.; Yao, Y.; Loomis, R. A.; Buhro, W. E. Methods for the ICP-OES Analysis of Semiconductor Materials. *Chem. Mater.* **2020,** *32*, 1760-1768.

For Table of Contents Only

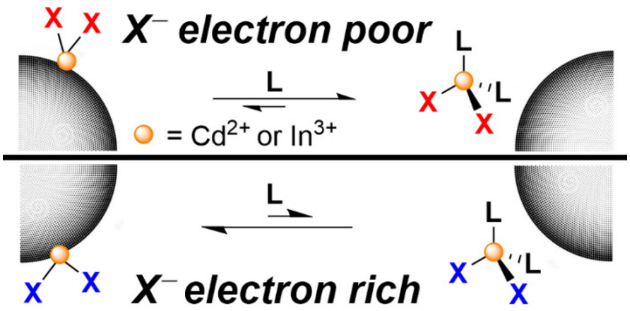

The $[Co(CO)_4]^-$ anion can substitute for the native anionic ligands of CdSe and InP nanocrystals and permits measurement of ligand dissociation by IR spectroscopy. Ligand displacement and association studies show that more Lewis acidic CdX_2 Z-type ligands are more readily displaced from nanocrystal surfaces by solvent or Lewis bases. Anion exchange between different metal cations is also shown to occur and to affect displaced ligands.